



# Hydro-geochemical evolution of groundwater in the central Yangtze River Basin, China

Meiyan Hu<sup>1</sup> · Peijiang Zhou<sup>1</sup> · Chaoqi Chen<sup>1</sup>

Accepted: 26 January 2023 / Published online: 12 February 2023

© The Author(s), under exclusive licence to Springer-Verlag GmbH Germany, part of Springer Nature 2023

## Abstract

Understanding the characteristics of groundwater hydro-chemical evolution is significant for better utilization and exploitation. In this study, principal component analysis, hydro-geochemical modeling and auxiliary chemical method were used to identify the hydro-chemical evolution in the groundwater of the central Yangtze River Basin. 17.02% of the groundwater samples had TH concentrations above the China national guideline. The relationship between the concentrations of  $\text{Ca}^{2+} + \text{Mg}^{2+}$  and  $\text{HCO}_3^-$  in phreatic groundwater and confined groundwater indicated that they may originate from the dissolution of the same carbonate minerals (such as dolomite and calcite minerals). Values of  $\delta^{18}\text{O}$  and  $\delta^2\text{H}$  in phreatic water (PGW) and confined water (CGW) suggested similar evolution process of the two aquifers.  $\delta^{18}\text{O}$  and  $\delta\text{D}$  in the mainstream of the Yangtze River presented an obvious enrichment trend along the flow direction. Principal component analysis indicated that the groundwater chemistry was mainly controlled by the anthropogenic activities and geological background. The groundwater evolution process of R2 and R3 appeared to be more similar. However, R3 was probably less affected by anthropogenic activities. The calculation results of mineral saturation index showed that calcite and dolomite were supersaturated in 96% of the groundwater at the area between the Yangtze River and Han River. This work not only strengthens the understanding of groundwater evolution in this area, but also provides a reference for groundwater analysis in other similar areas.

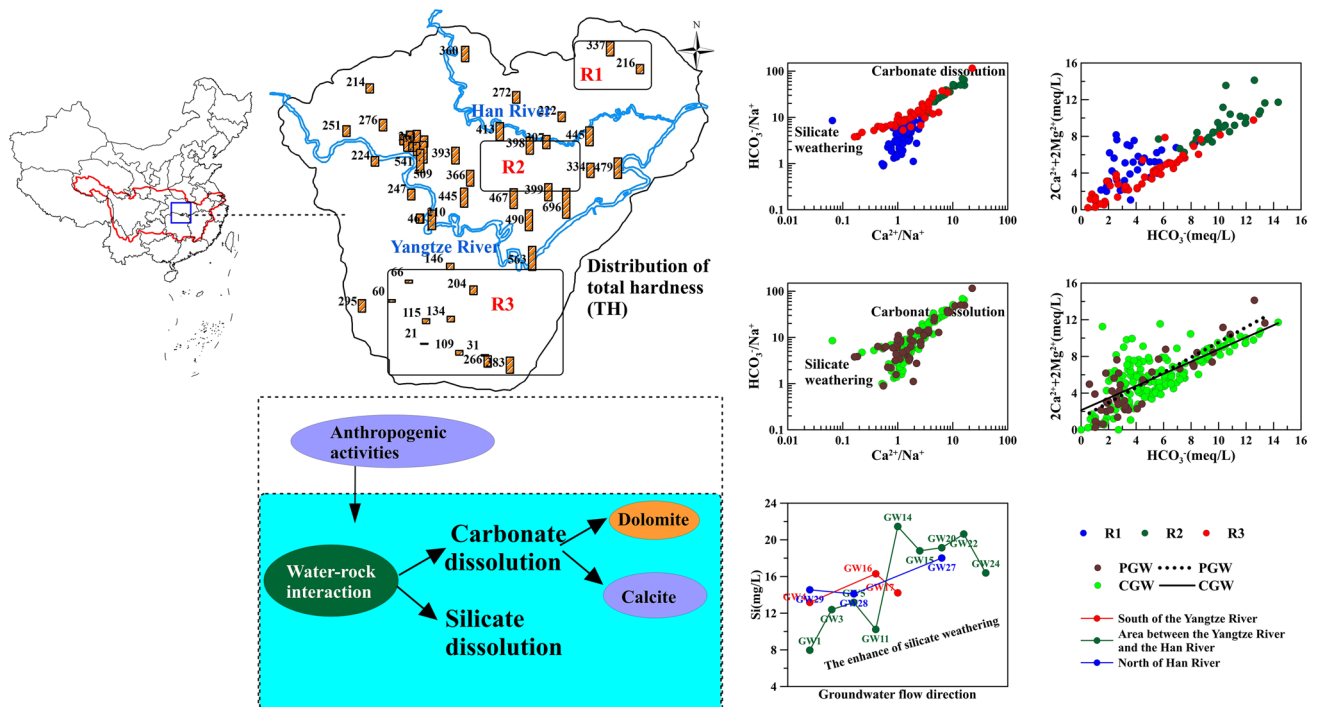
---

✉ Peijiang Zhou  
zhoupj@whu.edu.cn

✉ Chaoqi Chen  
chenchaoqi@whu.edu.cn

<sup>1</sup> School of Resource and Environmental Science, Hubei Biomass-Resource Chemistry and Environmental Biotechnology Key Laboratory, Eco-Environment Technology R&D and Service Center, Wuhan University, Wuhan 430079, People's Republic of China

## Graphical Abstract



**Keywords** Yangtze River · Hydro-geochemistry · Hydrogen and oxygen isotope · Principal component analysis · Geochemical modeling

## Introduction

High levels of total hardness in groundwater usually does not bring great harm and risk to human health, but the calcium ions in water are easily reacted with oxalic acid in drinking water during a long term, which leads to an increase in the incidence rate of kidney stones (Bondu et al. 2018). In addition, hard water can also lead to scale formation in pipes and kitchen utensils, which increase the consumption of fuel and detergent, resulting in economic burden. Hence, understanding the hydro-geochemical evolution and identifying its linkage with elevated total hardness in the study area would be a fascinating scientific output, along with its societal importance and environmental implications.

The chemical evolution of regional groundwater is mainly affected by natural factors (topography and climate), geological factors (lithological structure) and human factors (Gan et al. 2018). Many studies have proved that the differences of hydro-chemical characteristics can be used to indicate the geochemical evolution process (Awaleh et al. 2017; Barbieri et al. 2005; Liu et al. 2017; Pilla et al. 2006; Zheng et al.

2017; Zhu et al. 2007, 2008). Common methods include graphic method (such as Piper diagram (Huang and Wang 2018; Mountadar et al. 2018), Gibbs method (Gibbs 1970; Wen et al. 2005; Nazzal et al. 2014; Varol and Davraz 2014) and ion coefficient ratio (Ye et al. 2015).

In addition, hydrogen and oxygen isotope analysis (Khalil et al. 2015; Ayadi et al. 2018), multivariate statistical technique (Yidana et al. 2008; Rodriguez et al. 2016) and mineral saturation calculation (Gomaah et al. 2016; Slimani et al. 2017; Sharif et al. 2008) have been applied to study the chemical evolution of regional groundwater in recent years.

The central Yangtze River Basin is the main agricultural area in China, where the groundwater resources are very rich. Groundwater is the key source of agricultural and domestic water, the quality of groundwater is particularly important (Zhou et al. 2013). Due to the influence of regional geological background, water quality of some areas in the central Yangtze River Basin was affected by high iron, manganese and arsenic (Gan et al. 2014; Duan et al. 2015). Due to the influence of anthropogenic activities, the nitrate concentration in groundwater in this area had been increasing since 1992 (Niu et al. 2017). However, few scholars had systematically studied the controlling factors of groundwater Hydrochemistry in the central Yangtze River Basin so far.

Previously, some scholars analyzed the chemical characteristics of groundwater in some areas of the central Yangtze River Basin (Du et al. 2017; Zhou et al. 2013; Gan et al.

2014). However, these studies based on one region or one method had some limitations. More objective and comprehensive results would be got if various methods were combined. In this paper, the hydro-geochemical characteristics and controlling factors of shallow groundwater in the central Yangtze River Basin were systematically investigated and analyzed based on several methods. The results revealed the similarities and differences of groundwater chemistry under different sedimentary environment, which provided a basis for the study of other areas with similar hydrogeological conditions and guidance for better groundwater usage and possible management practice to improve groundwater quality in this area.

## Study area

The Yangtze River Basin is the third largest basin in the world, which spans the three economic regions of eastern, central and western China (Fig. 1a). The central Yangtze River Basin is an important agricultural production base in China with abundant natural resources (Fig. 1b). The crops planted are mainly rice, cotton, rapeseed and other cash crops. In addition, the industry in the central Yangtze River Basin is very well developed. Traditional competitive industries such as coal mining and washing, paper-making, textile and dyeing and chemical industry are the main development industries.

The study area contains several rivers and lakes, accounting for 36.5% of China's water resources (Deng et al. 2016; Liu and Wu 2016). The study area is located in the low plain area of the middle of the Yangtze River, which is composed of Jiangnan Plain and Dongting Lake Basin. The study area has a subtropical monsoon climate with abundant rainfall (Zhou et al. 2013).

The groundwater system in the central Yangtze River Basin can be divided vertically into different aquifers (Hu et al. 2022). Quaternary groundwater with shallow depth will be mainly studied in this paper, which can be divided into two groups of phreatic groundwater (PGW) and confined groundwater (CGW) (Du et al. 2017; Duan et al. 2015, 2017). The surface layer of the ground in study area is generally composed of a loose aquifer formed by alluvial facies, proluvial facies or lacustrine facies of Upper Pleistocene (Qp<sub>3</sub>) and Holocene (Qh) (Gan et al. 2014; 2018). The Quaternary loose sediments are deposited on the surface of the earth with a thickness ranging from 15 to 300 m, providing abundant storage and flow space for shallow groundwater. Quaternary sediments generally have a dual stratigraphic structure, with a clay/silt

layer overlying the sand layer (Fig. 1f). In the study area, the Quaternary sediments contain 29–50% of aluminum silicate minerals (montmorillonite, chlorite, illite and kaolinite) and 31–54% quartz (Gan et al. 2014). In addition, up to 20% of carbonate (calcite and dolomite) and albite were also detected in sandy sediments (Duan et al. 2015, 2017).

The flow direction of both surface water and groundwater are all from west to east. The groundwater is mainly recharged from rainfall and discharged to river water and adjacent aquifers or artificial wells (Du et al. 2017). Groundwater is discharged to the river in the dry season and recharged from the river in the wet season due to the interaction between the Yangtze River and the aquifers along the river (Yang et al. 2020).

In addition, three small regions in the area were studied (Fig. 1c–e). Region (R1) is located north to the Han River, having a piedmont deposit environment (Fig. 1c). Region (R2) is located between the Yangtze River and the Han River, having a fluvial alluvial environment (Fig. 1d). Region (R3) is located south to the Yangtze River, having a lacustrine sedimentation environment (Fig. 1e).

## Methodology

### Data preparation

The data involved in this study are shown in Table 1, including three data sets.

For the data set 1, 13 surface water and 47 groundwater samples, which were distributed in the central Yangtze River Basin, were collected or sampled to examine the chemical characteristics of surface water and groundwater (Table L1 and Table L2). The second data set included groundwater samples from the three areas of R1, R2 and R3 (Table L3, Table L4 and Table L5). Samples of R1 were self-collected, and data of R2 and R3 was obtained from the literature.

The samples in R1 were collected from September to October 2016, including 24 phreatic groundwater and 56 confined groundwater (Table L3). Routine anions and cations was determined by ion chromatography and ICP-AES in the Three Gorges Research Center for Geohazards, China University of Geosciences, and the detection limits were 0.01 mg/L and 0.001 mg/L, respectively. The samples were tested in Wuhan geological survey center of China Geological Survey, and the analysis error was less than 5%.

For the third data set, 26 surface water and 156 (78 for PGW and 78 for CGW) groundwater samples were collected to examine the hydrogen and oxygen isotopic composition of surface water and groundwater (Table L6, Table L7 and Table L8). Seventy-eight isotopic samples in R1 were sampled from September to October 2016 (the wet season).

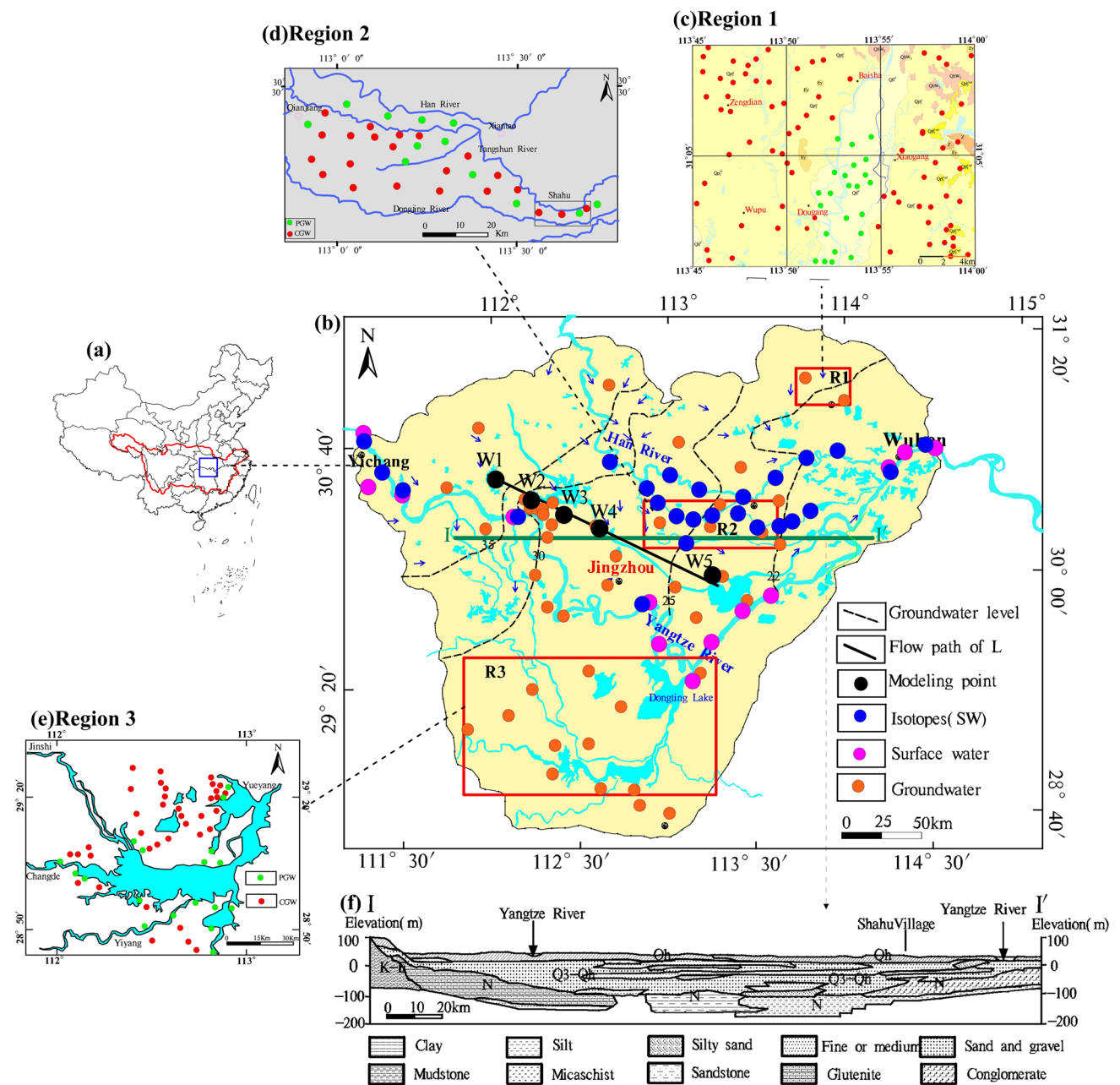


**Fig. 1** Location and sampling points distribution of **a** the Yangtze River Basin, **b** the middle of the Yangtze River, **c** Region1, **d** Region2, **e** Region3; hydrogeological profile; **f** I–I' (according to Gan et al. (2014))

Among them, 4 samples were sampled from SW, 55 from PGW and 19 from CGW. Hydrogen/oxygen (H/O) isotopes were measured using a gas stable isotope mass spectrometer (MAT253, Finnigan, Germany). The precisions for  $\delta^{18}\text{O}$  and  $\delta^2\text{H}$  were  $\pm 0.1\text{‰}$  and  $\pm 1.0\text{‰}$ , respectively.

### Data analysis

#### Chemical composition and hydrogen and oxygen isotopic composition analyses

The hydro-chemical and hydrogen–oxygen composition were analyzed using graphic method. Gibbs maps were often used to analyze the chemical genesis mechanism of groundwater. It can be qualitatively distinguished whether

**Table 1** Information of data collected in this study

Region	Type	<i>n</i>	Content	Time	Data source	Data set
The whole district	SW (river)	13	Surface water chemical composition	2013.07 (Wet)	Zhang et al. (2016)	Table L1
The whole district	GW	47	Groundwater chemical composition	2014–2019 (Wet)	Liu et al. (2021); Du et al. (2017); self-test; Yuan et al. (2021)	Table L2
R1	PGW	24	Groundwater chemical composition	2016 (Wet)	Self-test	Table L3
	CGW	56				
R2	PGW	12	Groundwater chemical composition	2015 (Wet)	Du et al. (2017)	Table L4
	CGW	22				
R3	PGW	18	Groundwater chemical composition	2019 (Wet)	Huang et al. (2021)	Table L5
	CGW	37				
The whole district	SW (river)	26	$\delta D/\delta^{18}O$	2013–2017 (Wet)	Wu et al. (2018); Du et al. (2017)	Table L6
R1/R2	PGW	78	$\delta D/\delta^{18}O$	2014–2017 (Wet)	Self-test; Du et al. (2017); Yu (2016)	Table L7
R1/R2	CGW	78	$\delta D/\delta^{18}O$	2014–2017 (Wet)	Self-test; Du et al. (2017); Gan et al. (2014); Yu (2016)	Table L8

the components of groundwater were mainly controlled by “evaporation concentration”, “water–rock interaction” or “rainfall” based on the Gibbs diagram of groundwater (Gibbs 1970; Gowrisankar et al. 2017).

In this study, chemical compositions were analyzed based on the 13 surface water and 47 groundwater samples in the whole study area. Spatial distribution of total hardness (TH) in the groundwater was graphed with ArcGIS (version 10.0). In addition, chemical compositions of R1 ( $n=80$ ), R2 ( $n=34$ ), R3 ( $n=55$ ), PGW ( $n=54$ ) and CGW ( $n=115$ ) were analyzed, respectively. The groundwater chemical characteristics in both phreatic aquifer groundwater (PGW) and confined aquifer groundwater (CGW) were compared. The isotopic composition was analyzed based on 26 surface water and 110 groundwater samples.

### Principal component analysis

The application of multivariate statistical analysis in the field of hydro-geochemical analysis can improve our understanding of the spatiotemporal pattern of groundwater geochemistry (Cloutier et al. 2008; Wang et al. 2015). Principal component or factor analysis (PCA or FA) is widely used in various research fields. In the study of hydro-geochemistry, PCA or FA can reduce the dimension of large data sets to analyze the potential factors affecting the chemical characteristics of groundwater in the area, determining the process of the evolution of groundwater chemistry and the sources of geological and anthropogenic pollutants (He et al. 2015; Kumar et al. 2021; Moeck et al. 2016; Moya et al. 2015).

Parameters with additive characteristics (such as Eh, EC, TDS and TH) and with above 5% missing data values (such as Si) were eliminated from the statistical analysis. 12 variables (pH,  $K^+$ ,  $Na^+$ ,  $Ca^{2+}$ ,  $Mg^{2+}$ ,  $HCO_3^-$ ,  $Cl^-$ ,  $SO_4^{2-}$ ,  $NO_3^-$ -N, Fe, Mn and As) were selected for principal component analysis.

In this study, IBM SPSS statistical software (version 20) was used to analyze the principal component analysis (PCA) of the groundwater chemistry based on the 47 groundwater samples in the whole study area. In addition, to explore the differences in the chemical composition of groundwater in three different regions (south of the Yangtze River, area between the Yangtze River and the Han River and north of the Han River) and two different aquifers of PGW and CGW, principal component factor analysis was carried out based on the groundwater samples in R1 ( $n=80$ ), R2 ( $n=34$ ), R3 ( $n=55$ ), PGW ( $n=54$ ) and CGW ( $n=115$ ), respectively.

### Saturation index calculation and hydro-geochemical modeling

Saturation index was a thermodynamic parameter which could be used to express the precipitation and dissolution state of the mineral phase (Rifai and El-Fiky 2003; Sharif et al. 2008; Slimani et al. 2017). It could be used to qualitatively predict the tendency of precipitation or dissolution of the mineral phase in water. Where  $SI = \log(IAP/K)$ , IAP is the ionic activity product and K is the equilibrium constant of minerals. When the SI value is less than zero, it indicates that the water and the target minerals are unsaturated, and dissolution might occur in



**Table 2** Chemical composition of the points on the simulation path

Sample No	pH	HCO <sub>3</sub> <sup>-</sup> (mg/L)	Ca <sup>2+</sup> (mg/L)	Cl <sup>-</sup> (mg/L)	F <sup>-</sup> (mg/L)	Mg <sup>2+</sup> (mg/L)	Na <sup>+</sup> (mg/L)	SO <sub>4</sub> <sup>2-</sup> (mg/L)
W1	7.82	327.15	52.91	7.68	0.32	18.56	30.44	1
W2	7.77	342.5	59.36	7.5	0.32	19.5	31.47	1
W3	7.77	370.36	80.96	8.07	0.17	22.85	14.07	1
W4	7.57	570.72	137.88	2.78	0.17	24.31	12.49	1
W5	7.5	546.43	133.87	5.56	0.12	20.91	12.49	1

the circulating water system. Whether SI is greater than zero can be used to judge whether the mineral is saturated.

The geochemical program PHREEQC based on the database phreeqc.dat was applied to calculate the saturation index. In this study, the mineral saturation index was analyzed based on the 47 groundwater samples in the whole study area. Spatial distribution of the main carbonate minerals (calcite and dolomite) was graphed with ArcGIS (version 10.0). In addition, saturation index of R1 ( $n=80$ ), R2 ( $n=34$ ), R3 ( $n=55$ ), PGW ( $n=54$ ) and CGW ( $n=115$ ) was calculated, respectively.

Hydro-geochemical modeling is a research method for quantitative analysis of hydro-geochemical processes, and the most commonly used model is inverse geochemical modeling. The purpose of inverse geochemical modeling is to determine the existence and transformation form of hydro-chemical components in the reaction path, which is more commonly used to calculate the amount of mineral transfer in the process of groundwater flow (Sharif et al. 2008; Bretzler et al. 2011). Based on the mass balance and charge balance reaction model, a hydro-geochemical evolution model is established to quantitatively calculate the mineral mass transfer from one location to another along the flow path, which can be expressed as follows:

$$\begin{cases} \sum_{p=1}^p a_p b_{p,k} = mT,K(\text{Ending}) - mT,K(\text{Starting}) \\ \sum_{p=1}^p u_p a_p = \Delta RS \end{cases} \quad (1)$$

To quantitatively analyze the water–rock interaction in the study area, PHREEQC was used to carry out geochemical inversion simulation. The groundwater flow path of L (W1–W5) was selected to analyze the water–rock interaction in the process of groundwater flow in the middle of the Yangtze River according to the groundwater contour map of the study area (Fig. 1b).

Sericite, quartz and a small amount of halite and fluorite were also found in the study area during the field investigation (Zeng 1997; Zhao 2005). Gypsum and halite were found in Jiangnan plain according to the statistical database of China's economic and social development. Based on the hydro-geochemistry, lithology and mineral constituents,

possible minerals such as calcite, dolomite, fluorite, gypsum and halite were selected. In addition, cation exchange reactions might occur in the groundwater system according to the distribution characteristics of cations. Based on the results of hydro-chemical test, seven elements of Na, Ca, Mg, C, S, F and Cl were taken as constraint variables. Models were established with the selected mineral phases and main target elements. The water chemical compositions of each point on the simulation path are shown in Table 2.

## Results

### Chemical and hydrogen and oxygen isotopic composition

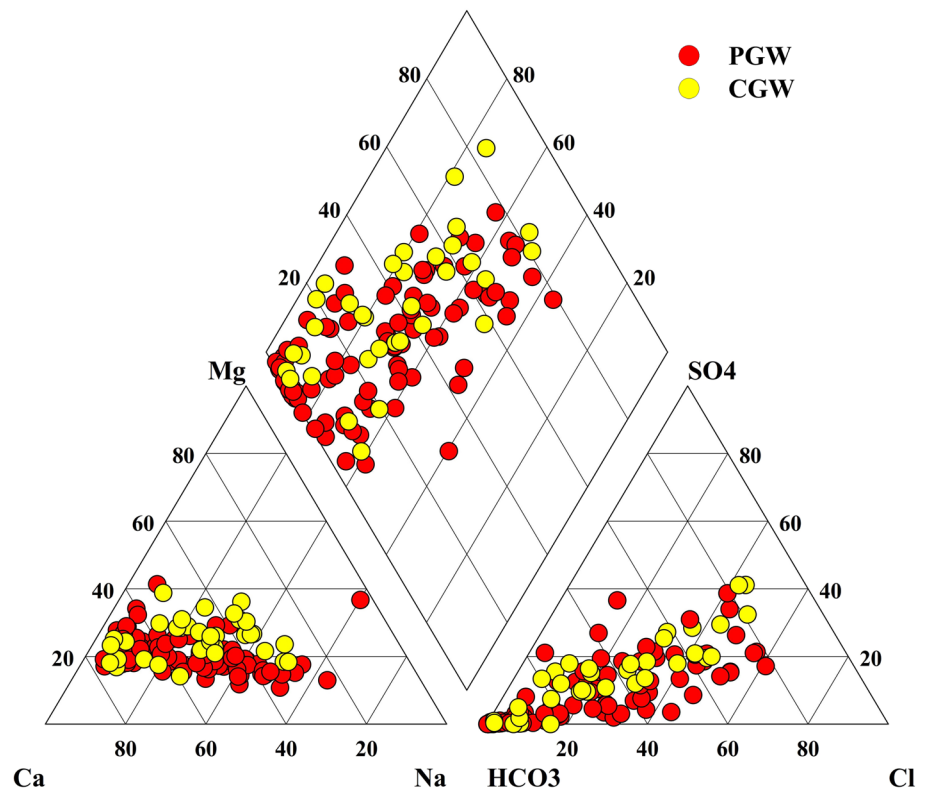
The concentrations of pH, TH, K<sup>+</sup>, Na<sup>+</sup>, Ca<sup>2+</sup>, Mg<sup>2+</sup>, HCO<sub>3</sub><sup>-</sup>, Cl<sup>-</sup>, SO<sub>4</sub><sup>2-</sup>, Fe, Mn and As of the surface water and groundwater of the central Yangtze River Basin are presented in Table 3. Compared to surface water, the pH values in the groundwater ranged more widely, which fluctuated in the range of 5.68–8.29 with a median value of 7.5. The median concentrations of Na<sup>+</sup>, Ca<sup>2+</sup>, Mg<sup>2+</sup> and HCO<sub>3</sub><sup>-</sup> in the groundwater were generally higher than that of the surface water. On the contrary, the levels of K<sup>+</sup>, Cl<sup>-</sup> and SO<sub>4</sub><sup>2-</sup> in groundwater were relatively lower than that of the surface water. The values of NO<sub>3</sub>-N in groundwater were low, with the median concentration value of 0.03 mg/L. Ca<sup>2+</sup> and HCO<sub>3</sub><sup>-</sup> were indicated as the dominant ions in the groundwater. The groundwater types were mainly HCO<sub>3</sub>-Ca type, HCO<sub>3</sub>-Ca-Mg type and HCO<sub>3</sub>-Ca-Na type (Fig. 2). The Mg equivalent percentages of K<sup>+</sup> + Na<sup>+</sup> and SO<sub>4</sub><sup>2-</sup> were lower than 25%.

The concentration distributions of groundwater Fe, Mn and As were extremely uneven and fluctuated from 0.001 mg/L to 28.68 mg/L, 0.01 mg/L to 3.43 mg/L, and below detection limit (BDL) to 762.3 mg/L, respectively. In particular, the concentration of arsenic was higher between the Yangtze River and the Han River. The total hardness (TH) levels of the surface water were generally lower than that of the groundwater, ranging from 51.17 mg/L to 142.25 mg/L and 20.83 mg/L to 695.88 mg/L, respectively. 17.02% of the 47 groundwater samples had TH

**Table 3** Basic chemical composition in surface water and groundwater

Index	Unit	Surface water (n=13)			Groundwater (n=47)		
		Min	Max	Median	Min	Max	Median
pH		7.51	8.61	7.93	5.68	8.29	7.5
K <sup>+</sup>	mg/L	1.6	9.5	2.9	0.64	41.66	1.76
Na <sup>+</sup>	mg/L	13.3	36.8	16.2	3.4	491.42	21.03
Ca <sup>2+</sup>	mg/L	16.3	44.4	37	4.4	329	86.57
Mg <sup>2+</sup>	mg/L	2.5	10.2	7	2.37	55.79	23
HCO <sub>3</sub> <sup>-</sup>	mg/L	47.25	73.8	64.19	51.14	730.41	370.36
Cl <sup>-</sup>	mg/L	7.4	37.5	14.8	0.85	77.46	11.12
SO <sub>4</sub> <sup>2-</sup>	mg/L	24.4	50.7	33.3	0.42	124.22	4.73
NO <sub>3</sub> -N	mg/L	–	–	–	0.002	20.55	0.03
Fe	mg/L	–	–	–	0.001	28.68	0.74
Mn	mg/L	–	–	–	0.01	3.43	0.098
As	mg/L	–	–	–	BDL	762.3	0.01
TH	mg/L	51.17	142.25	122.00	20.83	695.88	306.77

\*BDL means below detection limit

**Fig. 2** Projection of water samples in the Piper diagram

concentrations above the China national guideline (i.e., 450 mg/L) (MEP 1994), showing a trend of increasing gradually from northwest to southeast (Fig. 3a).

The TH levels were higher in the area between Yangtze River and Han River, which were mainly affected by the concentrations of Ca<sup>2+</sup>, Mg<sup>2+</sup> and HCO<sub>3</sub><sup>-</sup> in groundwater (Fig. 3a). The concentrations of TH, HCO<sub>3</sub><sup>-</sup>, Ca<sup>2+</sup> and

Mg<sup>2+</sup> in R2 were relatively higher than those at the other two zones (Fig. 3b–e). The relationship between the main ions in the water in the study area is shown in Fig. 4. The order of cations in all measured groundwater samples was shown as Ca<sup>2+</sup> > Mg<sup>2+</sup> > Na<sup>+</sup> + K<sup>+</sup>, and the anions appeared to be HCO<sub>3</sub><sup>-</sup> > Cl<sup>-</sup> > SO<sub>4</sub><sup>2-</sup> (Fig. 4a–i). The great positive correlation between Ca<sup>2+</sup> and Mg<sup>2+</sup> with Ca<sup>2+</sup> + Mg<sup>2+</sup> with

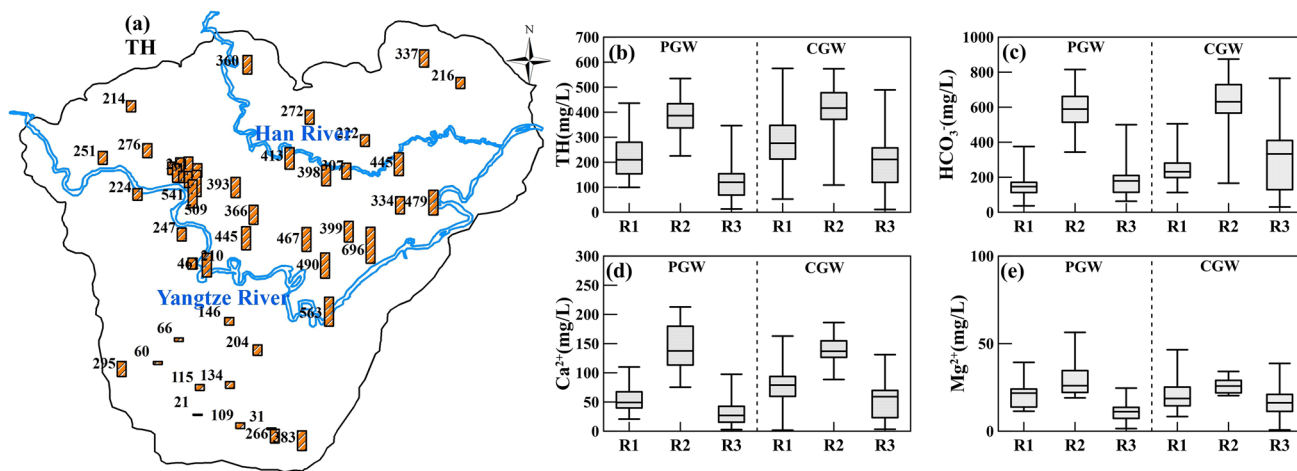


**Fig. 3** Distribution of **a** TH in the middle of the Yangtze River; box diagram of **b** TH, **c** HCO<sub>3</sub><sup>-</sup>, **d** Ca<sup>2+</sup> and **e** Mg<sup>2+</sup> in groundwater samples of R1,R2 and R3

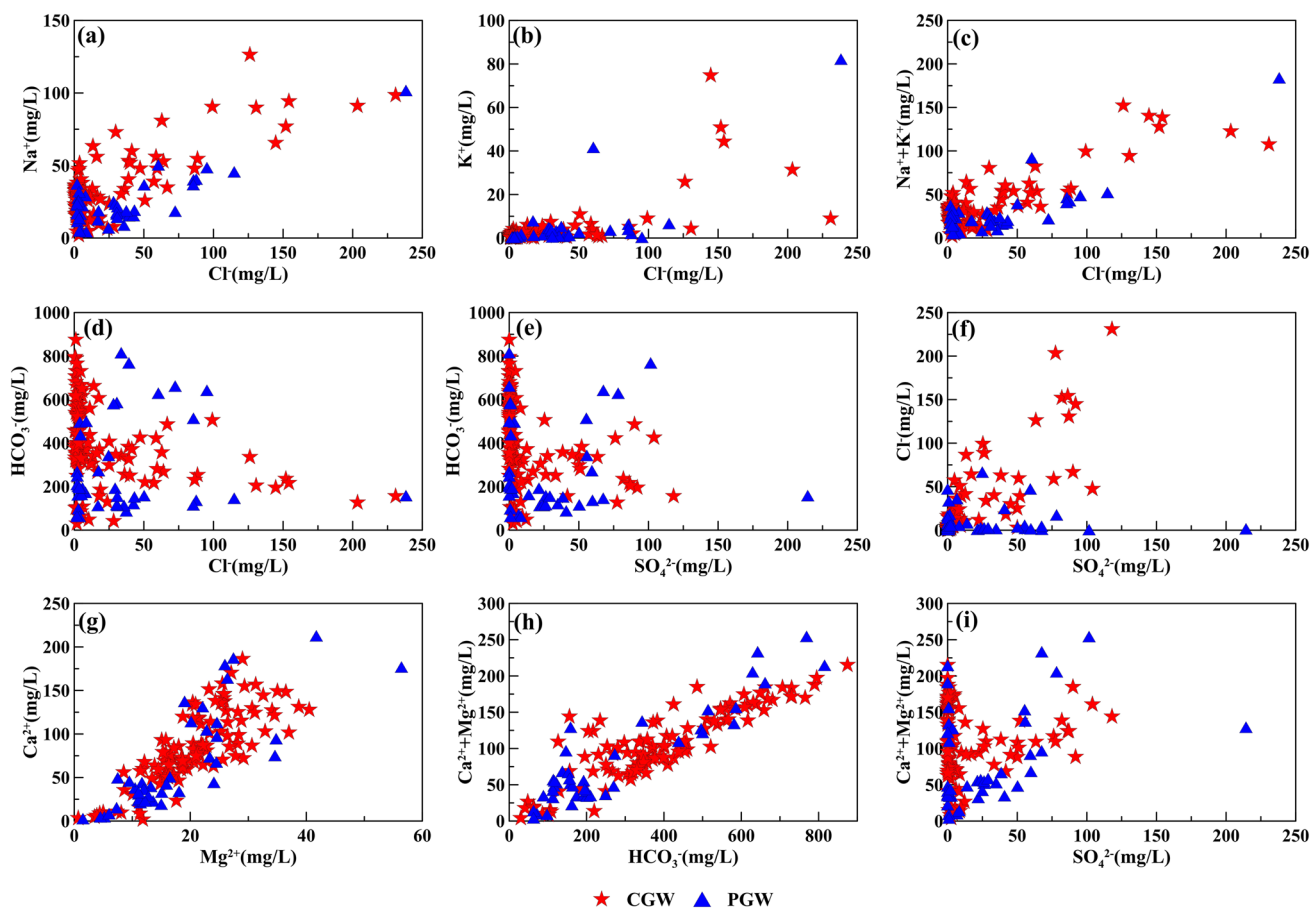


**Fig. 4** Relation between **a** Na<sup>+</sup> with Cl<sup>-</sup>, **b** K<sup>+</sup> with Cl<sup>-</sup>, **c** Na<sup>+</sup>+K<sup>+</sup> with Cl<sup>-</sup>, **d** HCO<sub>3</sub><sup>-</sup> with Cl<sup>-</sup>, **e** HCO<sub>3</sub><sup>-</sup> with SO<sub>4</sub><sup>2-</sup>, **f** Cl<sup>-</sup> with SO<sub>4</sub><sup>2-</sup>, **g** Ca<sup>2+</sup> with Mg<sup>2+</sup>, **h** Ca<sup>2+</sup>+Mg<sup>2+</sup> with HCO<sub>3</sub><sup>-</sup> and **(i)** Ca<sup>2+</sup>+Mg<sup>2+</sup> with SO<sub>4</sub><sup>2-</sup> in all groundwater samples

HCO<sub>3</sub><sup>-</sup> indicated that these might have common mineral sources (such as dolomite, CaMg (CO<sub>3</sub>)<sub>2</sub>) (Fig. 4g–h).

Cl<sup>-</sup> had a positive correlation with Na<sup>+</sup>+K<sup>+</sup>, but no obvious correlation with SO<sub>4</sub><sup>2-</sup> (Fig. 4e, f).



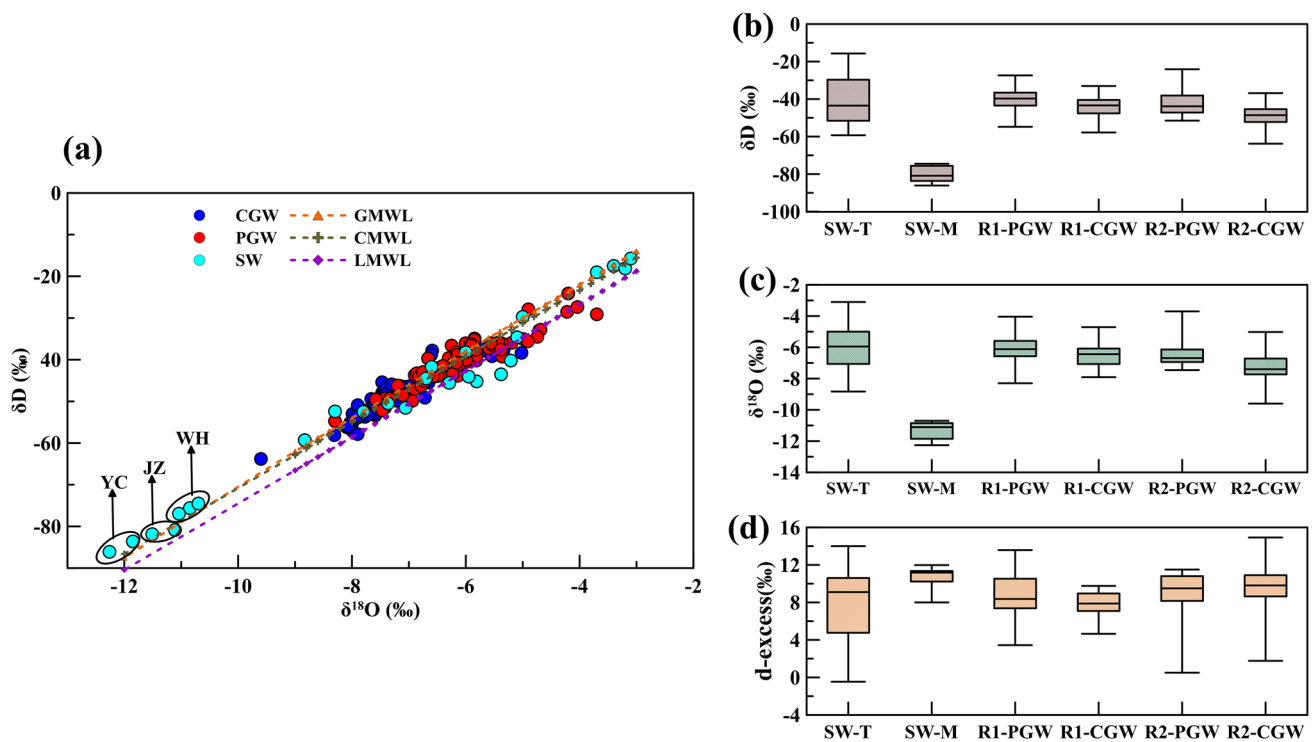


**Fig. 5** a Comparison of  $\delta D$  and  $\delta^{18}O$  in SW, PGW and CGW in the central of the Yangtze River. YC means Yichang, JZ means Jingzhou, WH means Wuhan. Comparison of **b**  $\delta D$ , **c**  $\delta^{18}O$  and **d** d-excess in different waters; SW-T means tributary river water, SW-M means

mainstream river water. The global meteoric water line (GMWL), China meteoric water line (CMWL) and local meteoric water line (LMWL) were referred to the values of Craig (1961), Zheng et al. (1983) and Zhang et al. (2008), respectively

Oxygen and hydrogen stable isotopes ( $\delta^{18}O$  and  $\delta D$ ) played a key role in the process of hydrological tracking. According to the previous studies, it was found that the slope of the local meteoric water line (LMWL,  $\delta D = 7.96 \delta^{18}O + 5.1$ ) LMWL was located below the China meteoric water line (CMWL,  $\delta D = 7.9 \delta^{18}O + 8.2$ ) (Fig. 5a). The average ratios of  $\delta^{18}O$  in surface water (SW), phreatic water (PGW) and confined water (CGW) in the study area were  $-7.37\text{‰}$ ,  $-6.17\text{‰}$  and  $-7.06\text{‰}$ , respectively, and the average ratios of  $\delta D$  were  $-50.47\text{‰}$ ,  $-40.70\text{‰}$  and  $-47.23\text{‰}$ , respectively (Fig. 5b-c). Based on the least square regression, the best fitting regression line parameters of different aquifers were calculated. The fitting equations of evaporation line for surface water (SW), phreatic water (PGW) and confined water (CGW) were:  $\delta D = 7.35 \delta^{18}O + 3.45$  ( $R^2 = 0.97$ ),  $\delta D = 6.43 \delta^{18}O - 1.07$  ( $R^2 = 0.88$ ) and  $\delta D = 6.70 \delta^{18}O + 0.04$  ( $R^2 = 0.90$ ). The tributaries of the Yangtze River were more enriched in  $\delta D$  and  $\delta^{18}O$  than the mainstream. In addition, the mainstream of the Yangtze River presented an obvious enrichment trend along the flow direction (Yichang-Jingzhou-Wuhan) (Fig. 5a). The d-excess in the mainstream of the Yangtze River was higher than that in other tributaries, indicating that its evaporation intensity was larger (Fig. 5d).

### Principal component analysis of groundwater

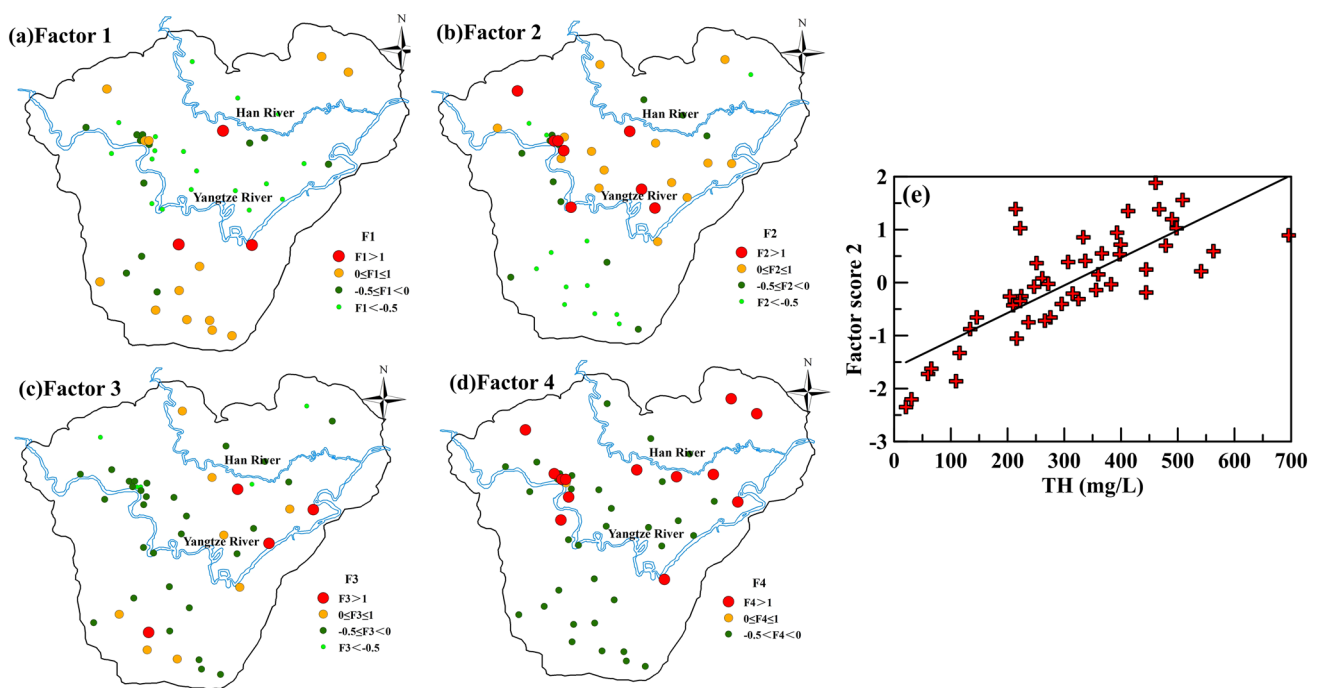
Principal component matrix and rotated factors matrix were obtained by principal component analysis and maximum variance orthogonal rotation based on the 47 groundwater samples in the whole study area. Four factors were extracted, explaining 77.2% of the total variance of the data set. The four factors account for 20.65, 20.61, 17.76 and 17.17% of the total variance (Table 4), respectively. All variables had communality values above 0.60 except for Fe, which meant that the factor solution could effectively explain most information of the original data set. Factor 1 was characterized by highly positive loadings in  $K^+$ ,  $NO_3-N$  and  $SO_4^{2-}$  and negative loadings in pH. Factor 2 was characterized by highly positive loadings in  $Ca^{2+}$ ,  $Mg^{2+}$  and  $HCO_3^-$ . Factor 3 was characterized by highly positive loadings in Fe, Mn and As. Factor 4 was characterized by highly positive loadings in  $Na^+$  and  $Cl^-$  (Table 4).

A large spatial heterogeneity was shown in both factor score 1 and factor score 3 (Fig. 6a, c). Factor score 2 and factor score 4 appeared to be higher in the north of the Yangtze River than those in the south of the Yangtze River (Fig. 6b, d). In particular, factor score 2 was more enriched at the area between Yangtze River and Han River (Fig. 6b). In addition,

**Table 4** Principal components loadings and rotation factor loading matrix (CGW,  $n=47$ )

Variables	Communality	Principal components loadings				Rotated factor loadings			
		PC1	PC2	PC3	PC4	Factor1	Factor2	Factor3	Factor4
pH	0.61	-0.18	-0.16	0.69	-0.29	-0.62	0.38	-0.25	0.14
K <sup>+</sup>	0.71	0.68	0.37	-0.32	-0.08	0.79	0.28	0.00	0.07
Na <sup>+</sup>	0.99	0.14	0.58	0.60	0.53	0.01	0.00	-0.02	0.99
Ca <sup>2+</sup>	0.92	0.85	-0.11	0.35	-0.27	0.23	0.91	0.14	0.13
Mg <sup>2+</sup>	0.65	0.65	-0.08	0.20	-0.43	0.22	0.77	-0.04	-0.06
HCO <sub>3</sub> <sup>-</sup>	0.87	0.59	-0.51	0.46	-0.24	-0.18	0.86	0.31	-0.05
Cl <sup>-</sup>	0.97	0.16	0.60	0.58	0.50	0.04	0.01	-0.04	0.98
SO <sub>4</sub> <sup>2-</sup>	0.53	0.43	0.55	-0.08	-0.19	0.58	0.23	-0.31	0.22
NO <sub>3</sub> -N	0.85	0.59	0.42	-0.57	-0.02	0.92	0.06	0.01	-0.03
Fe	0.33	0.12	-0.50	0.04	0.26	-0.20	0.09	0.52	-0.10
Mn	0.89	0.57	-0.38	-0.29	0.58	0.34	0.07	0.87	0.01
As	0.83	0.39	-0.57	-0.03	0.59	-0.02	0.11	0.90	0.04
Explained variance (%)	–	25.41	19.43	17.03	14.32	20.65	20.61	17.76	17.17
Cumulative of variance (%)	–	25.41	44.84	61.88	76.20	20.65	41.26	59.03	76.20

Significant loadings (absolute value > 0.70) are in italic

**Fig. 6** Spatial distribution of **a** factor score 1, **b** factor score 2, **c** factor score 3, and **d** factor score 4 in CGW of the whole study area

factor score 2 showed a significant positive correlation with total hardness ( $F2 = 0.0052 * TH - 1.61$  ( $R^2 = 0.61$ )) (Fig. 6e).

Four factors were extracted with cumulative contribution rates of 77.50% and 81.05% in R2 and R3, respectively, according to principal component factor analysis results of the three regions in the study area. However, three factors were extracted in R1, and the cumulative contribution rate was 75.00% (Table 5).

Principal component factor analysis result of the two aquifers showed that four factors were extracted in both PGW and CGW, with cumulative contribution rates of 76.24 and 84.34%, respectively (Table 6).

**Table 5** Results of PCA in R1, R2 and R3

Region	Type	Factor 1	Factor 2	Factor 3	Factor 4
R1 ( <i>n</i> = 80)	Variables	K <sup>+</sup> , Na <sup>+</sup> , Ca <sup>2+</sup> , Mg <sup>2+</sup> , Cl <sup>-</sup> , SO <sub>4</sub> <sup>2-</sup> , NO <sub>3</sub> -N	pH, HCO <sub>3</sub> <sup>-</sup> , Mn	Fe, As	
	Explained variance (%)	40.19	17.63	16.17	
R2 ( <i>n</i> = 34)	Variables	Na <sup>+</sup> , Ca <sup>2+</sup> , Mg <sup>2+</sup> , HCO <sub>3</sub> <sup>-</sup>	Cl <sup>-</sup> , SO <sub>4</sub> <sup>2-</sup> , NO <sub>3</sub> -N, Fe	pH, Mn, As	K <sup>+</sup>
	Explained variance (%)	27.46	22.98	14.35	12.71
R3 ( <i>n</i> = 55)	Variables	pH, Na <sup>+</sup> , Ca <sup>2+</sup> , Mg <sup>2+</sup> , HCO <sub>3</sub> <sup>-</sup>	Cl <sup>-</sup> , SO <sub>4</sub> <sup>2-</sup> , NO <sub>3</sub> -N	K <sup>+</sup> , Fe, As	Mn
	Explained variance (%)	30.48	19.25	19.00	12.33

**Table 6** Results of PCA in PGW and CGW

Aquifer	Type	Factor 1	Factor 2	Factor 3	Factor 4
PGW ( <i>n</i> = 54)	Variables	K <sup>+</sup> , Na <sup>+</sup> , Cl <sup>-</sup> , SO <sub>4</sub> <sup>2-</sup> , NO <sub>3</sub> -N	Ca <sup>2+</sup> , Mg <sup>2+</sup> , HCO <sub>3</sub> <sup>-</sup>	Fe, As	pH, Mn
	Explained variance (%)	33.66	20.38	12.30	9.90
CGW ( <i>n</i> = 115)	Variables	K <sup>+</sup> , Na <sup>+</sup> , Cl <sup>-</sup> , SO <sub>4</sub> <sup>2-</sup> , NO <sub>3</sub> -N	Ca <sup>2+</sup> , Mg <sup>2+</sup> , HCO <sub>3</sub> <sup>-</sup> , Fe	Mn, As	pH
	Explained variance (%)	37.29	22.61	15.79	8.64

### Saturation index and rock water–rock interaction

The distribution of mineral saturation index of calcite and dolomite was very similar (Fig. 7a, d). Calcite and dolomite were supersaturated in 96% of the groundwater at the area between the Yangtze River and Han River. However, mineral saturation of only 13.33% groundwater samples in the south of the Yangtze River was undersaturated (Fig. 7a, d), which was consistent with the calculation of R1, R2 and R3. The median values of saturation index and IAP of calcite and dolomite in R2 were higher than those in R1 and R3. In addition, the median values of saturation index and IAP of calcite and dolomite in CGW were higher than those in PGW (Fig. 7b, c, e, f). The concentration of Si in groundwater showed a gradual increasing trend along the groundwater flow direction, whether in the north of Han River, the south of Yangtze River or the area between Yangtze River and Han River (Fig. 7g, h).

Considering the obvious supersaturation of dolomite and calcite in the region between the Yangtze River and the Han River, inverse modeling was carried out along L path. The modeling results are shown in Table L9. Table 7 shows the calculated saturation index of the start and end points on the simulated path. The optimal solutions (Table 8) were selected considering the thermodynamic balance, element adsorption affinity, hydro-chemical evolution characteristics and mineral saturation index (Text S1). Both the precipitation of calcite, gypsum and halite and the dissolution of dolomite and Ca–Na cation exchange reaction occurred in the path (Fig. 8a–f). The precipitation of calcite along the path in the plain area between the Yangtze River and the Han River was obvious (Fig. 8a), which was consistent with the increasing trend of SI value of calcite along the path. The

SI value of calcite increased at first and then decreased in the process of groundwater runoff along the path (Table 7), which resulted in the gradual precipitation of calcite at first and the slow dissolution at W5 (Table 8, Fig. 8a). Dolomite was obviously dissolved along the groundwater flow of W2–W3–W4 (Fig. 8b). Gypsum and halite showed precipitation trend in the path. The Ca–Na cation exchange reaction mainly occurred in the path W2–W3–W4 (Fig. 8e–f).

## Discussion

### Affecting factors of groundwater hydro-chemical evolution

The groundwater chemistry was affected by many factors, such as anthropogenic activities, water–rock interaction and groundwater residence time within the aquifer (Halim et al. 2010; Mukherjee et al. 2009; Verma et al. 2016). This was also verified by the results of principal component analysis. Positive correlation between SO<sub>4</sub><sup>2-</sup> and NO<sub>3</sub>-N (*p* < 0.001, Table L10) demonstrated that SO<sub>4</sub><sup>2-</sup> may have the same origin with NO<sub>3</sub>-N (Fig. 9b, e). SO<sub>4</sub><sup>2-</sup> was usually considered to be sourced from anthropogenic activities (Niu et al. 2017). This was also confirmed by the fact that the levels of SO<sub>4</sub><sup>2-</sup> in groundwater were relatively lower than that of the surface water (Table 3). As NO<sub>3</sub>-N and SO<sub>4</sub><sup>2-</sup> in groundwater of the central Yangtze River Basin most probably resulted from the anthropogenic input (Liang et al. 2020; Niu et al. 2017), factor 1 was defined as anthropogenic activities.

The contents of silicate minerals and carbonate minerals were as high as 55–77% and 20% in the central Yangtze River Basin (Duan et al. 2017). Silicate weathering and

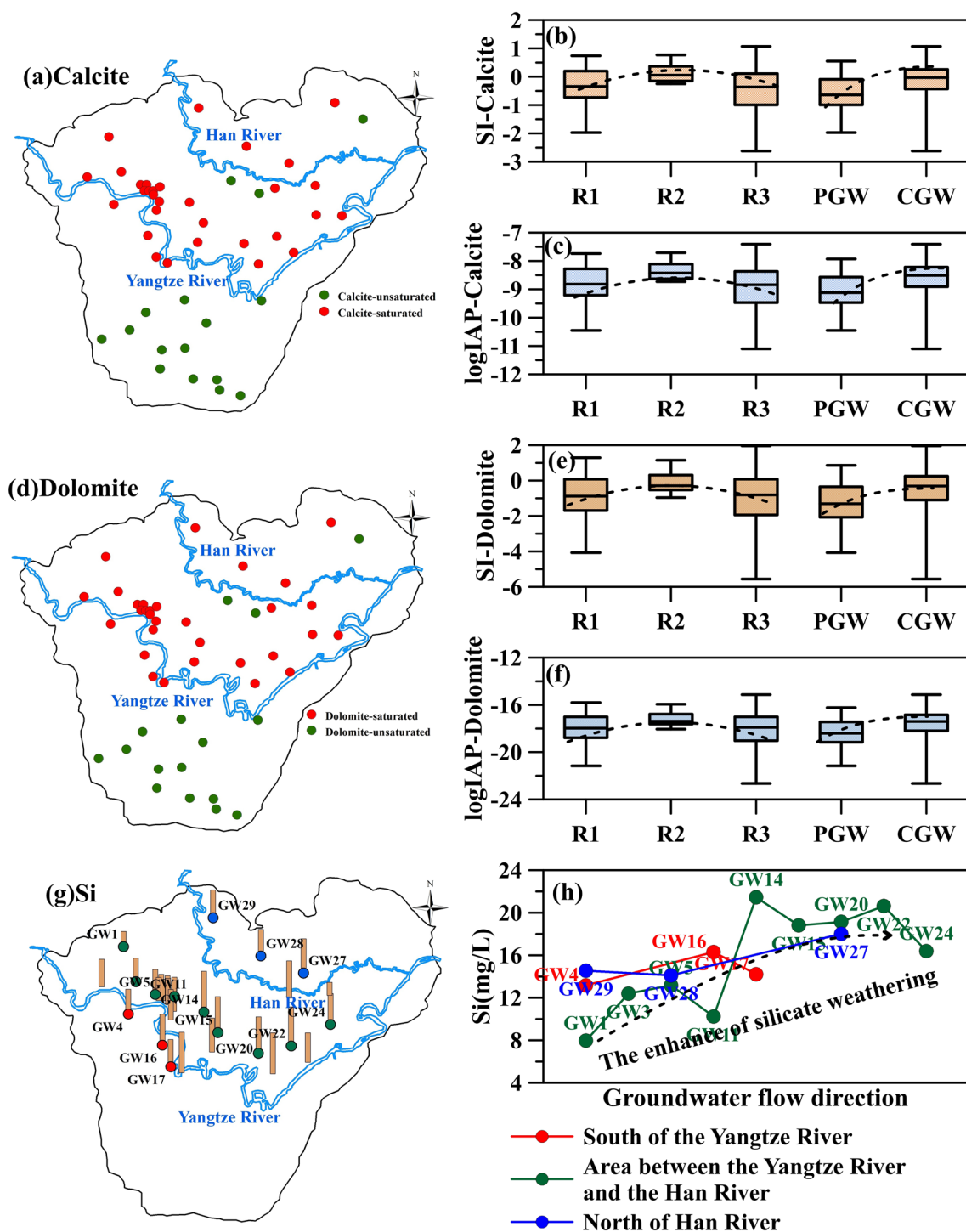


**Fig. 7** Distribution of saturation index of **a** calcite and **d** dolomite; saturation index and IAP of **b**, **c** calcite and **e**, **f** dolomite. Distribution of **g** groundwater and **h** trend along the groundwater direction

carbonate dissolution played an important role in Quaternary groundwater. (Gaillardet et al. 1999). High concentrations of bicarbonate and calcium in shallow groundwater were typical characteristics of groundwater affected by water-carbonate mineral interactions (Du et al. 2017; Hu and Zhou

2021; Zhou et al. 2013). The varying trend of  $\text{HCO}_3^-$  and  $(\text{Ca}^{2+} + \text{Mg}^{2+})$  mg equivalent concentration was very consistent (Fig. 10c, f). Most of  $\text{Ca}^{2+}$ ,  $\text{Mg}^{2+}$  and  $\text{HCO}_3^-$  came from the dissolution of carbonate. Factor 2 represented the intensity of groundwater carbonate interaction (Table 6).

**Table 7** SI value of the points on the simulation path

Sample No.	Calcite	Dolomite	Gypsum	Fluorite	Halite
W1	0.66	1.22	-3.70	-2.13	-8.19
W2	0.68	1.22	-3.67	-2.09	-8.19
W3	0.83	1.46	-3.57	-2.52	-8.17
W4	1.00	1.60	-3.43	-2.34	-9.05
W5	0.91	1.36	-3.43	-2.65	-8.74

**Table 8** Optimal solutions

Phase	<i>L</i>			
	W1–W2	W2–W3	W3–W4	W4–W5
	$\times 10^{-6}$	$\times 10^{-6}$	$\times 10^{-5}$	$\times 10^{-6}$
Calcite	–	–	–	–98.7
Dolomite	–	138	6.01	–
Fluorite	–	–	–	–1.32
Gypsum	–	–3.95	–	–
Halite	–	–	–43.1	–
CaX <sub>2</sub>	–24.9	378	–18.1	–
NaX	49.9	–757	36.3	–

Factor 3 represented the redox conditions, since these variables generally occurred in reducing conditions. The strength of reduction conditions significantly controlled the behavior of Fe and As in groundwater (Schaefer et al. 2016). A positive correlation between  $\text{Cl}^-$  with  $\text{Na}^+ + \text{K}^+$  ( $p < 0.001$ ) demonstrated that  $\text{Cl}^-$  may have the same origin with  $\text{Na}^+ + \text{K}^+$  (Fig. 9a, d).  $\text{Na}^+$  generally originated from weathering and dissolution of silicate or feldspar,

which indicated that  $\text{Cl}^-$  and  $\text{Na}^+ + \text{K}^+$  were more likely to originate from mineral dissolution. Factor 4 was defined as the intensity of groundwater–silicate interaction (Table 4). Gradual increasing trend of concentration of Si along the groundwater flow direction (Fig. 7g, h) indicated that silicate dissolution gradually increased.

### Hydro-chemical evolution relationship between R1, R2 and R3

The principal component analysis results of R2 and R3 appeared to be more similar (Table 5), which may indicate that the conditions of groundwater in the two regions were more similar (Mertler and Reinhart. 2016; Gan et al. 2018). Factor 1 and factor 2 in R2 and R3 reflected the water–rock interaction and the influence of anthropogenic activities, respectively, and factor 3 and factor 4 represented the metal ions such as Fe, Mn and As. The principal component analysis result of R1 was different from that of the other two areas (Table 5). It may indicate that there was a great difference between the groundwater environment of the alluvial plain area (R1) in the south of Han River and fluvial and lake-facies deposition area (R2 and R3) in the north of Han River. The concentrations of  $\text{Cl}^-$ ,  $\text{SO}_4^{2-}$  and  $\text{NO}_3\text{-N}$  in groundwater of R3 were significantly lower than those of R1 and R2 (Fig. 9a, b, c). It probably related to the less influence of anthropogenic activities in R3.

Different water–rock reactions happened in groundwater due to the influence of the geological background of aquifer in the process of groundwater flow. The relationship between  $\text{Ca}^{2+}/\text{Na}^+$  with  $\text{HCO}_3^-/\text{Na}^+$  and  $\text{Mg}^{2+}/\text{Na}^+$  in the three regions showed a higher intensity of carbonate dissolution in R2 (Fig. 10a, b), resulting in the higher concentration of

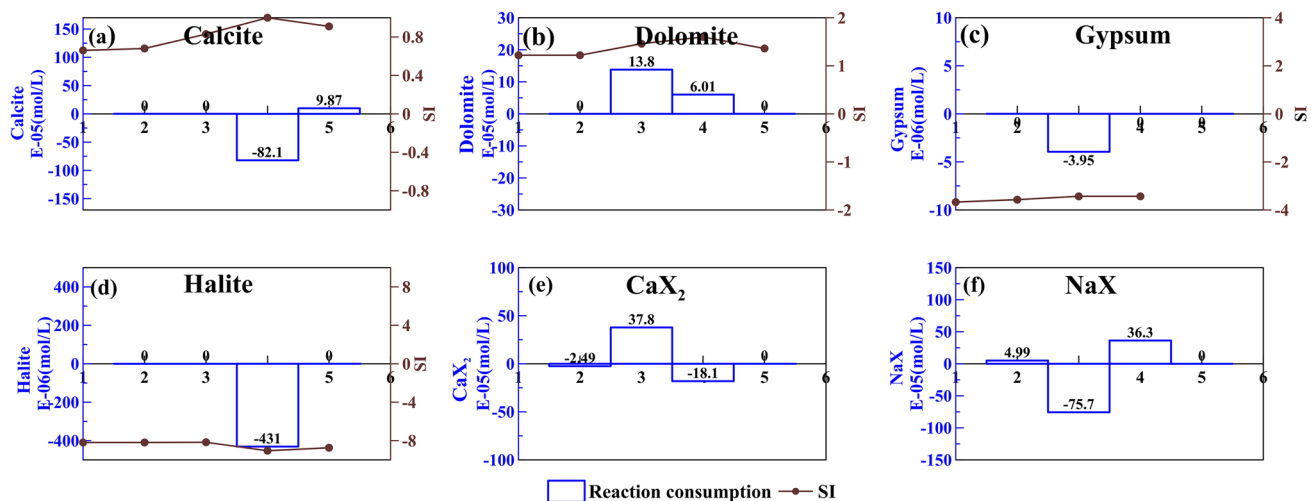


**Fig. 8** Water–rock reaction diagram in three flow paths of **a** calcite, **b** dolomite, **c** gypsum, **d** halite, **e** CaX<sub>2</sub>, **f** NaX (“–” represent precipitation; “+” represent dissolution)



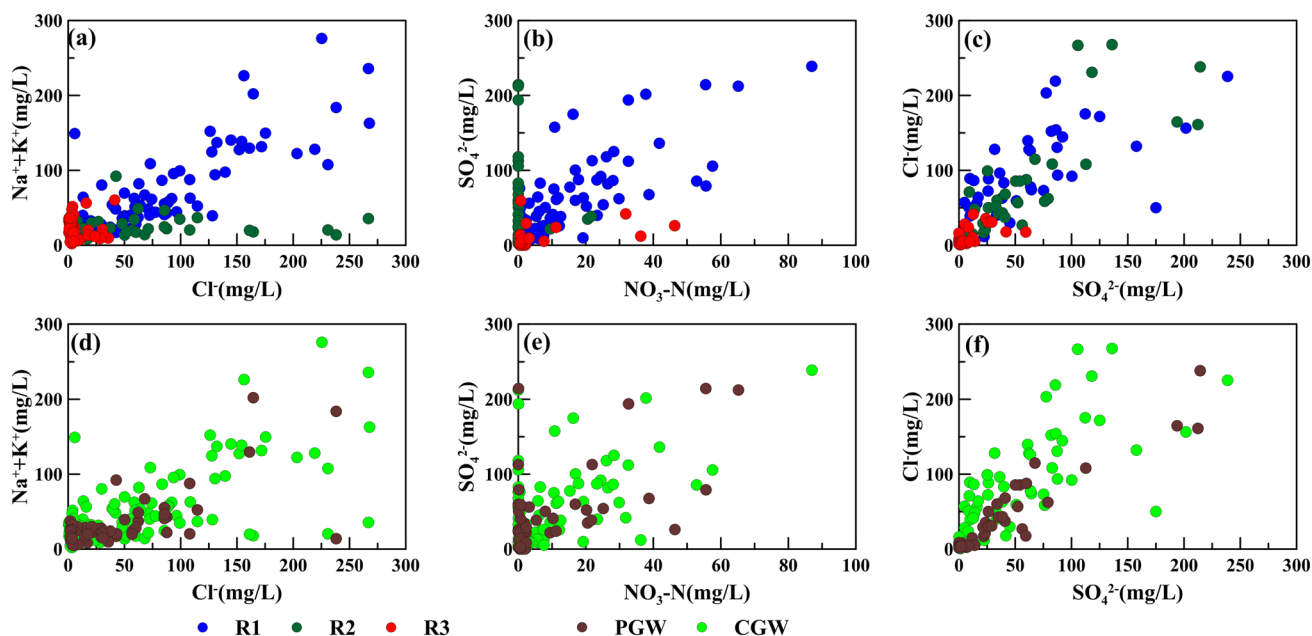


**Fig. 9** Relation between  $\text{Na}^+ + \text{K}^+$  vs  $\text{Cl}^-$  in **a** R1, R2 and R3 and **d** PGW, CGW. Relation between  $\text{SO}_4^{2-}$  vs  $\text{NO}_3\text{-N}$  in **b** R1, R2 and R3 and **e** PGW, CGW. Relation between  $\text{Cl}^-$  vs  $\text{SO}_4^{2-}$  in **c** R1, R2 and R3 and **f** PGW, CGW

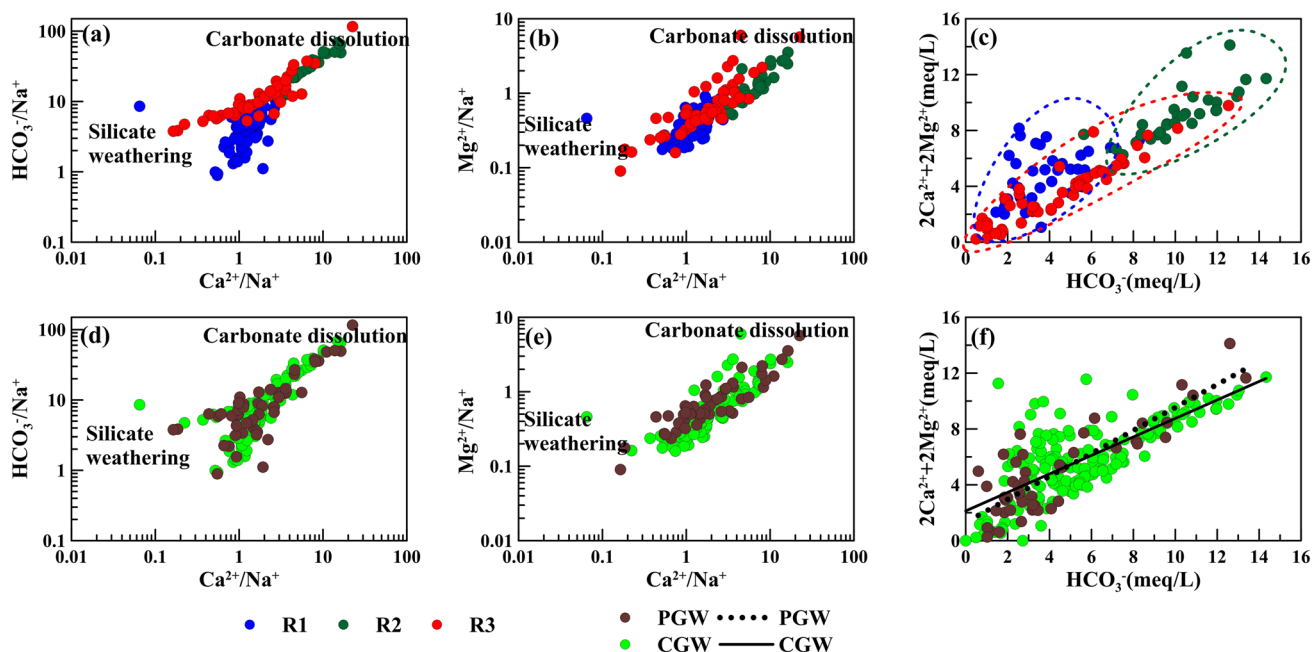


**Fig. 10** Relationship between  $\text{Ca}^{2+}/\text{Na}^+$  and  $\text{HCO}_3^-/\text{Na}^+$  in **a** R1, R2, R3 and **b** PGW, CGW. Relationship between  $\text{Ca}^{2+}/\text{Na}^+$  and  $\text{Mg}^{2+}/\text{Na}^+$  in **c** R1, R2, R3 and **d** PGW, CGW. Relationship between  $\text{HCO}_3^-$  and  $\text{Ca}^{2+} + \text{Mg}^{2+}$  in **e** R1, R2, R3 and **f** PGW, CGW

$\text{HCO}_3^-$  and  $\text{Ca}^{2+} + \text{Mg}^{2+}$  in R2 (Fig. 10c). The ratios of  $\text{Na}^+ / (\text{Na}^+ + \text{Ca}^{2+})$  and  $\text{Cl}^- / (\text{Cl}^- + \text{HCO}_3^-)$  of most groundwater samples in three regions of the study area were less than 0.5, indicating that the main chemical components of groundwater mainly came from the interaction of mineral and water,

and the influence of environmental geological background played a leading role (Fig. 11a-b). When the TDS concentration in groundwater was the same, the ratios of  $\text{Na}^+ / (\text{Na}^+ + \text{Ca}^{2+})$  and  $\text{Cl}^- / (\text{Cl}^- + \text{HCO}_3^-)$  in the R2 area were the lowest, which may also reflect that R2 was more affected

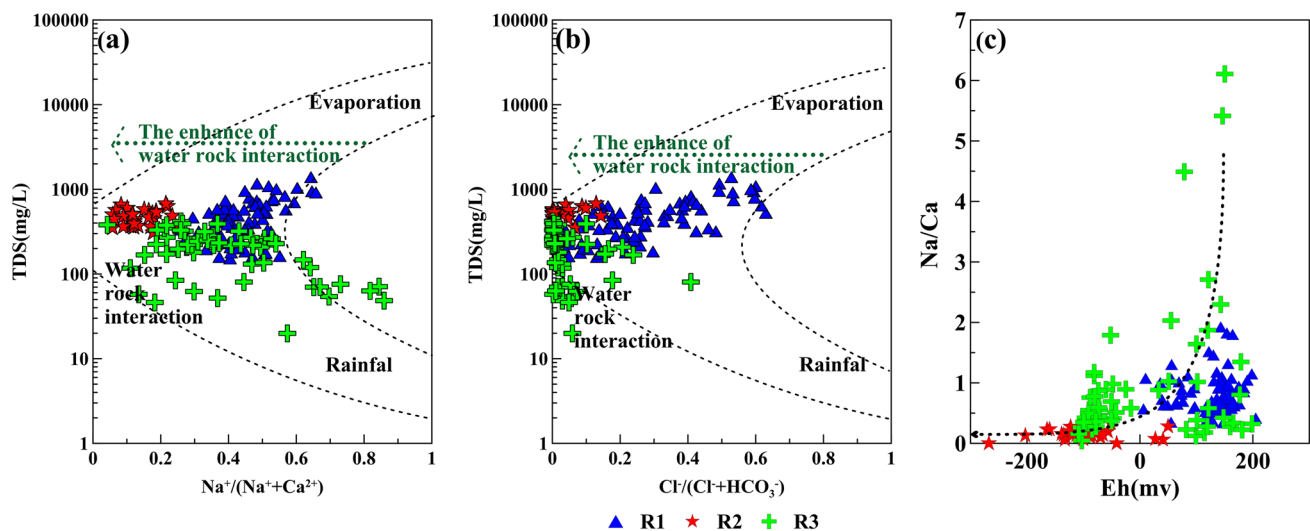


**Fig. 11** Relation between TDS vs **a**  $Na^+/Na^+ + Ca^{2+}$  and **b**  $Cl^-/Cl^- + HCO_3^-$  in R1, R2 and R3; relation between **c**  $Na^+/Ca^{2+}$  vs Eh in R1, R2 and R3

by water–rock interaction (Fig. 11a–b). The higher median values of saturation index and IAP of calcite and dolomite in R2 (Fig. 7a, d) also demonstrated it. The increase of calcium concentration and decrease of sodium concentration may be caused by ion exchange and the continuous dissolution of carbonate rocks in the process of groundwater flow (Fig. 11c). Meanwhile, the redox potential decreased with the oxidation of reducing minerals such as dissolved organic matter and sulfide during the chemical evolution of groundwater (Gascoyne 2004; Ryan et al. 2013).

### Hydro-chemical evolution relationship between PGW and CGW

The principal component results of PGW and CGW were very similar (Table 6). Four factors were extracted in both PGW and CGW. Factor 1 and factor 2 reflected the influence of anthropogenic activities and the water–rock interaction, respectively. Factor 3 and factor 4 represented the metal ions such as Fe, Mn, As and acid alkalinity, respectively. The groundwater evolution process of PGW and CGW was very similar (Zhou et al. 2013).

Ratios between  $Na^+ + K^+$  vs  $Cl^-$ ,  $SO_4^{2-}$  vs  $NO_3-N$  and  $Cl^-$  vs  $SO_4^{2-}$  in PGW were very consistent with those in CGW (Fig. 9d, e, f). In addition, the values of  $\delta^{18}O$  and  $\delta^2D$  and evaporation intensity (K) in PGW were similar to that in CGW (Fig. 5). It probably related to the close hydraulic connection between the two aquifers. Relationship between  $Ca^{2+}/Na^+$  with  $HCO_3^-/Na^+$  and  $Mg^{2+}/Na^+$  in the three regions did not show much difference in PGW and CGW (Fig. 10d, e). It was found that the fitting lines in the

two aquifers were almost the same when the Mg equivalent concentrations of  $(Ca^{2+} + Mg^{2+})$  and  $HCO_3^-$  in the two aquifers were fitted (Fig. 10e). It may be inferred that the same water carbonate reaction occurred in the two aquifers. However, the higher of the median values of saturation index and IAP of calcite and dolomite in CGW (Fig. 7b, c, e, f) showed a slightly higher intensity of carbonate dissolution in CGW, which resulted in a slightly higher concentration of  $HCO_3^-$  and  $Ca^{2+} + Mg^{2+}$  in CGW (Fig. 10f).

### Conclusion

The hydro-chemical evolution and hydrogen and oxygen isotopic composition of groundwater in the central Yangtze River Basin (China) have been studied using different methods. The chemical types of groundwater in the study area were mainly  $HCO_3-Ca$  type,  $HCO_3-Ca-Mg$  type and  $HCO_3-Ca-Na$  type. The median concentrations of  $Na^+$ ,  $Ca^{2+}$ ,  $Mg^{2+}$  and  $HCO_3^-$  in the groundwater were generally higher than that of the surface water. On the contrary, levels of  $K^+$ ,  $Cl^-$  and  $SO_4^{2-}$  in groundwater were relatively lower than that of the surface water. 17.02% of the groundwater samples had TH concentrations above the China national guideline. The ratios of  $\delta^{18}O$  and  $\delta D$  in phreatic water (PGW) were close to those in confined water (CGW). In addition, the mainstream of the Yangtze River presented an obvious enrichment trend of  $\delta^{18}O$  and  $\delta D$  along the flow direction.

Principal component analysis indicated that the groundwater chemistry was mainly controlled by the anthropogenic activities and geological background. The groundwater evolution process of PGW and CGW was very similar.

The intensity of carbonate dissolution in CGW was a litter higher than that of PGW. The groundwater evolution process of R2 and R3 appeared to be more similar. However, R3 was probably less affected by anthropogenic activities. The calculation results of mineral saturation index showed that calcite and dolomite were supersaturated in 96% of the groundwater at the area between the Yangtze River and Han River. The inverse modeling results also showed that water carbonate interaction occurred obviously in the regional groundwater between the two rivers. R2 was more affected by water–rock interaction. In addition, silicate dissolution gradually increased along the groundwater flow direction.

**Supplementary Information** The online version contains supplementary material available at <https://doi.org/10.1007/s13146-023-00852-2>.

**Acknowledgements** This research was supported by the National High Technology Research and Development Program of China (No. 2007AA06Z418), the National Natural Science Foundation of China (Nos. 20577036, 20777058, 20977070), the National Natural Science Foundation of Hubei province in China (No. 2015CFA137), and the Open Fund of Hubei Biomass-Resource Chemistry and Environmental Biotechnology Key Laboratory, and the Fund of Eco-environment Technology R&D and Service Center (Wuhan University).

**Author contribution** MH: writing, review and editing. PZ: review and editing. CC: review and editing.

**Data availability** All relevant data are included in the paper or Supplementary Information.

## Declarations

**Conflict of interest** The authors declare that they have no known competing financial interests or personal relationships that could have appeared to influence the work reported in this paper.

## References

- Awaleh MO, Baudron P, Soubaneh YD, Boschetti T, Hoch FB, Egueh NM, Gassani J (2017) Recharge, groundwater flow pattern and contamination processes in an arid volcanic area: insights from isotopic and geochemical tracers (Bara aquifer system, Republic of Djibouti). *J Geochem Explor* 175:82–98
- Ayadi Y, Mokadem N, Besser H, Khelifi F, Harabi S, Hamad A, Hamed Y (2018) Hydrochemistry and stable isotopes ( $\delta^{18}\text{O}$  and  $\delta^2\text{H}$ ) tools applied to the study of karst aquifers in southern mediterranean basin (Teboursouk area, NW Tunisia). *J Afr Earth Sc* 137:208–217
- Barbieri M, Boschetti T, Petitta M, Tallini M (2005) Stable isotope ( $^2\text{H}$ ,  $^{18}\text{O}$  and  $^{87}\text{Sr}/^{86}\text{Sr}$ ) and hydrochemistry monitoring for groundwater hydrodynamics analysis in a karst aquifer (Gran Sasso, Central Italy). *Appl Geochem* 20(11):2063–2081
- Bondu R, Cloutier V, Rosa E (2018) Occurrence of geogenic contaminants in private wells from a crystalline bedrock aquifer in western Quebec, Canada: geochemical sources and health risks. *J Hydrol* 559:627–637
- Bretzler A, Osenbruck K, Gloaguen R, Ruprecht JS, Kebede S, Stadler S (2011) Groundwater origin and flow dynamics in active rift systems—A multi-isotope approach in the Main Ethiopian Rift. *J Hydrol* 402(3–4):274–289
- Cloutier V, Lefebvre R, Therrien R, Savard MM (2008) Multivariate statistical analysis of geochemical data as indicative of the hydro-geochemical evolution of groundwater in a sedimentary rock aquifer system. *J Hydrol* 353(3–4):294–313
- Craig H (1961) Isotope variation in meteoric waters. *Science* 133:1702–1703
- Deng K, Yang S, Lian E, Li C, Yang C, Wei H (2016) Three Gorges Dam alters the Changjiang (Yangtze) river water cycle in the dry seasons: evidence from HO isotopes. *Sci Total Environ* 562:89–97
- Du Y, Ma T, Deng YM, Shen S, Lu ZJ (2017) Sources and fate of high levels of ammonium in surface water and shallow groundwater of the Jiangnan Plain, Central China. *Environ Sci Processes Impact* 19(2):161–172
- Duan YH, Gan YQ, Wang YX, Deng YM, Guo XX, Dong CJ (2015) Temporal variation of groundwater level and arsenic concentration at Jiangnan Plain, central China. *J Geochem Explor* 149:106–119
- Duan YH, Gan YQ, Wang YX, Liu CX, Yu K, Deng YM, Zhao K, Dong CJ (2017) Arsenic speciation in aquifer sediment under varying groundwater regime and redox conditions at Jiangnan Plain of Central China. *Sci Total Environ* 607:992–1000
- Gaillardet J, Dupré B, Louvat P, Allegre CJ (1999) Global silicate weathering and CO<sub>2</sub> consumption rates deduced from the chemistry of large rivers. *Chem Geol* 159(1–4):3–30
- Gan YQ, Wang YX, Duan YH, Deng YM, Guo XX, Ding XF (2014) Hydrogeochemistry and arsenic contamination of groundwater in the Jiangnan Plain, central China. *J Geochem Explor* 138:81–93
- Gan YQ, Zhao K, Deng YM, Liang X, Ma T, Wang YX (2018) Groundwater flow and hydrogeochemical evolution in the Jiangnan Plain, central China. *Hydrogeol J* 26(5):1609–1623
- Gascoyne M (2004) Hydrogeochemistry, groundwater ages and sources of salts in a granitic batholith on the Canadian Shield, southeastern Manitoba. *Appl Geochem* 19(4):519–560
- Gibbs RJ (1970) Mechanisms controlling world water chemistry. *Science* 170(3962):1088–1090
- Gomaah M, Meixner T, Korany EA, Garamoon H, Gomaa MA (2016) Identifying the sources and geochemical evolution of groundwater using stable isotopes and hydrogeochemistry in the Quaternary aquifer in the area between Ismailia and El Kassara canals Northeastern Egypt. *Arab J Geosci* 9(6):437
- Gowrisankar G, Jagadeshan G, Elango L (2017) Managed aquifer recharge by a check dam to improve the quality of fluoride-rich groundwater: a case study from southern India. *Environ Monit Assess* 189:200
- Halim MA, Majumder RK, Nessa SA, Hiroshiro Y, Sasaki K, Saha BB, Jinno K (2010) Evaluation of processes controlling the geochemical constituents in deep groundwater in Bangladesh: spatial variability on arsenic and boron enrichment. *J Hazard Mater* 180(1–3):50–62
- He J, Ma J, Zhao W, Sun S (2015) Groundwater evolution and recharge determination of the Quaternary aquifer in the Shule River basin Northwest China. *Hydrogeol J* 23(8):1745–1759
- Hu M, Zhou P, Chen C (2022) Spatial and temporal distribution and affecting factors of iron and manganese in the groundwater in the middle area of the Yangtze River Basin, China. *Environ Sci Pollut Res* 29:61204–61221
- Hu M, Zhou P (2021) Hydro-geochemical evolution characteristics of shallow groundwater in northeast of Jiangnan Plain China. *Carbonates Evaporites* 36(4):1–15
- Huang P, Wang X (2018) Piper-PCA-Fisher recognition model of water inrush source: a case study of the Jiaozuo mining area. *Geofluids* 2018:1–10
- Huang Y, Du Y, Ma T, Deng Y, Tao Y, Xu Y, Leng Z (2021) Dissolved organic matter characterization in high and low

- ammonium groundwater of Dongting Plain, central China. *Eco-toxicol Environ Saf* 208:111779
- Khalil MM, Tokunaga T, Yousef AF (2015) Insights from stable isotopes and hydrochemistry to the quaternary groundwater system, south of the Ismailia canal Egypt. *J Hydrol* 527:555–564
- Kumar S, Joshi SK, Pant N et al (2021) Hydrogeochemical evolution and groundwater recharge processes in arsenic enriched area in central Gangetic plain India. *App Geochem* 131:105044
- Liang Y, Ma R, Wang Y, Wang S, Qu L, Wei W, Gan Y (2020) Hydrogeological controls on ammonium enrichment in shallow groundwater in the central Yangtze River Basin. *Sci Total Environ* 741:140350
- Liu Y, Wu G (2016) Hydroclimatological influences on recently increased droughts in China's largest freshwater lake. *Hydrol Earth Syst Sci* 20(1):93–107
- Liu S, Tang Z, Gao M, Hou G (2017) Evolutionary process of saline-water intrusion in Holocene and Late Pleistocene groundwater in southern Laizhou Bay. *Sci Total Environ* 607:586–599
- Liu HH, Yang J, Ye M, James SC, Tang ZH, Dong J, Xing TJ (2021) Using t-distributed stochastic neighbor embedding (t-SNE) for cluster analysis and spatial zone delineation of groundwater geochemistry data. *J Hydrol* 597:126146
- Mertler CA, Reinhart RV (2016) *Advanced and multivariate statistical methods: practical application and interpretation*, 6th edn. Routledge, New York
- Ministry of Environmental Protection of the People's Republic of China, (1994). National Quality Standard for Ground Water (GB/T 14848–93) (in Chinese)
- Moeck C, Radny D, Borer P, Rothardt J, Auckenthaler A, Berg M, Schirmer M (2016) Multicomponent statistical analysis to identify flow and transport processes in a highly-complex environment. *J Hydrol* 542:437–449
- Mountadar S, Younsi A, Hayani A, Siniti M, Tahiri S (2018) Groundwater salinization process in the coastal aquifer sidi abedouled ghanem (province of el Jadida, Morocco). *J Afr Earth Sc* 147:169–177
- Moya CE, Raiber M, Taulis M, Cox ME (2015) Hydrochemical evolution and groundwater flow processes in the Galilee and Eromanga basins, Great Artesian Basin, Australia: a multivariate statistical approach. *Sci Total Environ* 508:411–426
- Mukherjee A, Bhattacharya P, Shi F, Fryar AE, Mukherjee AB, Xie ZM, Bundschuh J (2009) Chemical evolution in the high arsenic groundwater of the Huhhot basin (Inner Mongolia, PR China) and its difference from the western Bengal basin (India). *Appl Geochem* 24(10):1835–1851
- Nazzal Y, Ahmed I, Al-Arifi NSN et al (2014) A pragmatic approach to study the groundwater quality suitability for domestic and agricultural usage, Saq aquifer, northwest of Saudi Arabia. *Environ Monit Assess* 186(8):4655–4667
- Niu B, Wang H, Loáiciga HA, Hong S, Shao W (2017) Temporal variations of groundwater quality in the Western Jiangnan Plain, China. *Sci Total Environ* 578:542–550
- Pilla G, Sacchi E, Zuppi G, Braga G, Ciancetti G (2006) Hydrochemistry and isotope geochemistry as tools for groundwater hydrodynamic investigation in multilayer aquifers: a case study from Lomellina, Po plain, South-Western Lombardy Italy. *Hydrogeol J* 14(5):795–808
- Rifai R, El-fiky A (2003) Hydrogeochemical and diagenetic evolution of the safa sandstone formation, North Sinai Egypt. *J Sedimentol Soc Egypt* 11:239–261
- Rodríguez M, Sfer A, Sales A (2016) Application of chemometrics to hydrochemical parameters and hydrogeochemical modeling of Calera River basin in the Northwest of Argentina. *Environ Earth Sci* 75(6):500
- Ryan PC, Kim JJ, Mango H, Hattori K, Thompson A (2013) Arsenic in a fractured slate aquifer system, New England, USA: influence of bedrock geochemistry, groundwater flow paths, redox and ion exchange. *Appl Geochem* 39:181–192
- Schaefer MV, Ying SC, Benner SG, Duan Y, Wang Y, Fendorf S (2016) Aquifer arsenic cycling induced by seasonal hydrologic changes within the Yangtze River Basin. *Environ Sci Technol* 50(7):3521–3529
- Sharif MU, Davis RK, Steele KF, Kim B, Kresse TM, Fazio JA (2008) Inverse geochemical modeling of groundwater evolution with emphasis on arsenic in the Mississippi River Valley alluvial aquifer, Arkansas (USA). *J Hydrol* 350(1–2):41–55
- Slimani R, Guendouz A, Trolard F, Moulla AS, Hamdi-Aïssa B, Bourrié G (2017) Identification of dominant hydrogeochemical processes for groundwaters in the Algerian Sahara supported by inverse modeling of chemical and isotopic data. *Hydrol Earth Syst Sci* 21(3):1669–1691
- Varol S, Davraz A (2014) Assessment of geochemistry and hydrogeochemical processes in groundwater of the Tefenni plain (Burdur/Turkey). *Environ Earth Sci* 71(11):4657–4673
- Verma S, Mukherjee A, Mahanta C, Choudhury R, Mitra K (2016) Influence of geology on groundwater–sediment interactions in arsenic enriched tectono-morphic aquifers of the Himalayan Brahmaputra river basin. *J Hydrol* 540:176–195
- Wang H, Jiang X, Wan L, Han G, Guo H (2015) Hydro-geochemical characterization of groundwater flow systems in the discharge area of a river basin. *J Hydrol* 527:433–441
- Wen X, Wu Y, Su J, Zhang Y, Liu F (2005) Hydrochemical characteristics and salinity of groundwater in the Ejina Basin Northwestern China. *Environ Geol* 48(6):665–675
- Wu H, Li J, Song F, Zhang Y, Zhang H, Zhang C, He B (2018) Spatial and temporal patterns of stable water isotopes along the Yangtze River during two drought years. *Hydrol Process* 32(1):4–16
- Yang J, Ye M, Tang ZH, Jiao T, Song XY, Pei YZ, Liu HH (2020) Using cluster analysis for understanding spatial and temporal patterns and controlling factors of groundwater geochemistry in a regional aquifer. *J Hydrol* 583:124594
- Ye C, Zheng M, Wang Z, Hao W, Wang J, Lin X, Han J (2015) Hydrochemical characteristics and sources of brines in the Gasikule salt lake, Northwest Qaidam Basin China. *Geochem J* 49(5):481–494
- Yidana SM, Ophori D, Banoeng-Yakubo B (2008) A multivariate statistical analysis of surface water chemistry data—The Ankobra Basin Ghana. *J Environ Manag* 86(1):80–87
- Yu K (2016) The sources and influences of dissolved organic matter on temporal variations of groundwater arsenic concentrations: a case study in Jiangnan Plain, (Doctoral dissertation). China University of Geosciences, Wuhan (in Chinese)
- Yuan RQ, Zhong YX, Long XT (2021). Comprehensive evaluation of shallow groundwater quality in the upper plain of the Dongting Lake, (in Chinese). *Water Resources Protection*.1–9. <http://kns.cnki.net/kcms/detail/32.1356.TV.20201209.1237.005.html>
- Zhang L, Chen ZY, Nie ZL, Liu FL, Jia YK, Zhang XY (2008) Correlation between  $\delta^{18}\text{O}$  in precipitation and surface air temperature on different time-scale in China. *Nucl Sci Tech* 31:715–720 (in Chinese with English abstract)
- Zhang Y, Gan Y, Li X, Liu Y, Yu K, Zhang B (2016) Water chemical characteristics and controlling factors of the Yangtze River in the wet season, 2013. *Resour Environ Yangtze Basin* 25(4):645–654 (in Chinese with English Abstract)
- Zhao D (2005) The three-dimensional numerical simulation for groundwater system in Jiangnan Plain, (master's thesis). China University of Geosciences, Wuhan (in Chinese)
- Zheng SH, Hou FG, Ni BL (1983) The studies of hydrogen and oxygen stable isotopes in atmospheric precipitation in China. *Chin Sci Bull* 13:801–806 (in Chinese)
- Zheng Z, Zhang H, Chen Z, Li X, Zhu P, Cui X (2017) Hydrogeochemical and isotopic indicators of hydraulic fracturing flowback fluids in shallow groundwater and stream water, derived from dameigou

- shale gas extraction in the northern qaidam basin. *Environ Sci Technol* 51(11):5889–5898
- Zhou Y, Wang YX, Li YL, Zwahlen F, Boillat J (2013) Hydrogeochemical characteristics of central Jiangnan Plain China. *Environ Earth Sci* 68(3):765–778
- Zhu GF, Li ZZ, Su YH, Ma JZ, Zhang YY (2007) Hydrogeochemical and isotope evidence of groundwater evolution and recharge in Minqin Basin, Northwest China. *J Hydrol* 333(2–4):239–251
- Zhu GF, Su YH, Feng Q (2008) The hydrochemical characteristics and evolution of groundwater and surface water in the Heihe River Basin, northwest China. *Hydrogeol J* 16(1):167–182

**Publisher's Note** Springer Nature remains neutral with regard to jurisdictional claims in published maps and institutional affiliations.

Springer Nature or its licensor (e.g. a society or other partner) holds exclusive rights to this article under a publishing agreement with the author(s) or other rightsholder(s); author self-archiving of the accepted manuscript version of this article is solely governed by the terms of such publishing agreement and applicable law.